Atmospheric Pollution Research 9 (2018) 322–332

HOSTED BY

Contents lists available at ScienceDirect

Atmospheric Pollution Research

journal homepage: www.elsevier.com/locate/apr

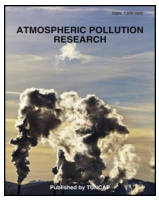

Low-cost methodology to estimate vehicle emission factors

J. Madrazo[a,*], A. Clappier[b]

[a] Swiss Federal Institute of Technology of Lausanne, Laboratory of Geographical Information Systems, Lausanne, Switzerland
[b] Université de Strasbourg, Laboratoire Image Ville Environnement, Strasbourg, France

ARTICLE INFO

Keywords:
Real-world emission factor
Street canyon
Traffic source
Roadside measurements
Emission factor uncertainties

ABSTRACT

Road traffic emission factors (EFs) are important parameters in managing air quality. Estimation typically requires data from advanced (and expensive) monitoring systems which remain unavailable in some regions (e.g. in developing countries). In this context, the use of simpler (lower-cost) systems may be more appropriate, but it is essential to guarantee the robustness of EF estimations. This article describes a methodology designed to estimate vehicle EFs from street canyon measurements of traffic fluxes, wind speed and direction, and pollutant concentration levels by using low-cost devices, all samples at a one-minute interval. We use different moving window filters (time periods) to average the raw measurements. Applying standard multiple linear regressions (MRL) and principal component regressions (PCR), we show that there is an optimal smoothing level that best relates traffic episodes and pollutant concentration measurements. An application for PM_{10}'s EFs on four vehicle categories of Havana's fleet shows a preference for PCR over MLR techniques since it reduced the collinearity effects that appear when traffic fluxes are naturally correlated between vehicle categories. The best regression fits ($R > 0.5$ and standard deviation of estimates $< 15\%$) were obtained by averaging data between 40′ and 60'; within the boundaries of 95% confidence interval motorcycles have an EF = 111.1 ± 2.7 mg km^{-1} veh^{-1}; modern, light vehicles have an EF = 90.6 ± 11.2 mg km^{-1} veh^{-1}; old, light vehicles have an EF = 125.4 ± 18.5 mg km^{-1} veh^{-1} and heavy vehicles have an EF = 415.1 ± 31.2 mg km^{-1} veh^{-1}. We showed that upgrading old light vehicles is a promising scenario for reducing PM_{10} air pollution in Havana by between 10 and 17%.

1. Introduction

Vehicle traffic is an important contributor to air pollution in many urban areas (Huang et al., 2016; Wang et al., 2017). Sound policy decisions on the control and management of traffic-related pollution depend on a reliable emission inventory and the emission characteristics of the vehicle fleet (Smit et al., 2017). Among others, one important parameter to be evaluated is the emission factor (EF) (Zarate et al., 2007); it characterizes the amount of pollutant emitted per mass of fuel consumed (fuel-based), per distance driven (task-based) or per energy used (task-based) (Brimblecombe et al., 2015). The EF can differ from one country to another depending on vehicle maintenance, driving patterns and fuel brands. More specifically, in developing countries, traffic flow is heterogeneous in nature (Jaikumar et al., 2017), and in most cases, exhaust emission standards fail to represent the real-world emissions from vehicles in these regions.

Different methods have been developed to estimate vehicle EFs. They typically require data from advanced monitoring systems (cf. Amato et al., 2016; Borrego et al., 2016; Ferm and Sjöberg, 2015; Keuken et al., 2016; Pang et al., 2014); chassis dynamometer tests (Jung et al., 2017; Li et al., 2013; Nakashima and Kajii, 2017; Pang et al., 2014) and on-road methods (Ait-Helal et al., 2015; Kam et al., 2012) are useful for providing accurate information about individual vehicle contributions. Both are often costly and time-consuming, and the number of testable vehicles (i.e., sample size) is limited. Approaches using measurements from road tunnels (Brimblecombe et al., 2015; Riccio et al., 2016; Zhang et al., 2015) and street canyons (Belalcazar et al., 2010; Klose et al., 2009; Vardoulakis et al., 2003) consider the contribution of the fleet in "real-world" driving conditions. Their basic principles are based on a statistical analysis of traffic and concentration episodes under specific pollutant dispersion rates.

In road tunnel studies, airflow conditions are well defined (i.e., by active mechanical ventilation systems or piston effects). Instead, problems might arise from the long pollutant residence time since receptor devices capture both the concentrations generated by passing vehicles and those retained, which could result in an overestimation of emission rates (Gertler et al., 1991). Additionally, if the instruments become saturated, they may not effectively capture the concentration peaks,

Peer review under responsibility of Turkish National Committee for Air Pollution Research and Control.
* Corresponding author. EPFL ENAC IIE LASIG, GC D2 416 (Bâtiment GC), Station 18, CH-1015 Lausanne, Suisse.
E-mail address: jessie.madrazo@epfl.ch (J. Madrazo).

http://dx.doi.org/10.1016/j.apr.2017.10.006
Received 7 June 2017; Received in revised form 10 October 2017; Accepted 18 October 2017
Available online 28 October 2017

and consequently, the EF results are underestimated (Brimblecombe et al., 2015). In street canyon studies, even if natural ventilation is reduced by the presence of buildings, the rate at which the street exchanges air with the atmosphere is greater, and the pollutant residence time is shorter compared to road tunnel studies, especially for the larger-sized particles that are greatly affected by gravity. In addition, wind flows are primarily controlled by micro-meteorological effects of urban geometry and dispersion phenomena, such as the mechanical turbulence induced by moving vehicles, and the atmospheric stability conditions are widely studied (e.g., Berkowicz and Danmark, 1997; Huang et al., 2016; Kakosimos et al., 2010; Kastner-Klein et al., 2003; Ketzel et al., 2000; Moradpour et al., 2017; Sokhi et al., 2008).

In this work, we use basic assumptions previously documented in other street canyon studies to estimate EFs. Testing different moving window filters (time periods) to average the raw measurements, we show the optimal smoothing levels that best relate traffic episodes and pollutant concentration measurements. To do that, we collected traffic counts and average concentration measurements for one-minute time steps. The pollutant dispersion is also quantified in one-minute steps by modelling changes (low-cost estimation) on meteorological and traffic constraints.

In section 2, we start with a brief description of the measurement campaign: data collection and processing. In section 3, we explain the methodology, detailing the most important assumptions for estimating EFs. The results of a case study are presented in section 4 (EFs of particulate matter -PM_{10}-for Havana's vehicle fleet); then, we assess the performances of the methodology used for different averaging times. Finally, in section 5, we discuss the effect of changing PM_{10} EF values under several abatement scenarios.

2. Sampling location and data

For this study, we examine data obtained over a 10-day measurement campaign in Havana in summer 2015. Data collection occurred in an urban canyon (see Fig. 1: Simon Bolivar Street with west-east direction). Data include traffic volume, wind speed and direction, and PM_{10} concentration levels.

Traffic was recorded on videotapes and then manually counted at a temporal resolution of 1′. The fleet of vehicles was classified into four clearly identifiable categories, i.e., motorcycles; modern light-duty cars (post-1980s); old light-duty cars (pre-1980s and of Russian or American origin); and heavy vehicles, including buses and trucks. No visual differentiation could be made in terms of technology or fuel system injection since many cars have been modernized with new parts (e.g., engines and disk brakes).

Wind speed and direction data were automatically registered from an IRDAM – WST7000C anemometer placed on the roof of the highest building (at a height of 13.6 m) within a 1-km radius; any other accurate meteorological station could be used. PM_{10} concentrations were recorded using a Thermo-Scientific ADR 1500 profiler (a low-cost device based on a highly sensitive light-scattering photometer technique) installed at a height of 1.5 metres on the southern side of the street canyon.

3. Methods

3.1. Basic assumptions

Due to the short distances between sources and receptors inside street canyons, only very fast chemical reactions significantly influence the measured concentrations (Berkowicz and Danmark, 1997). This enables us to ignore the chemical transformations of slowly reacting gases. Therefore, a linear relationship between released emissions and measured concentrations is valid (Palmgren et al., 1999), leading to the following equation:

$$C^t = D^t E^t + C_0^t \quad (1)$$

where C^t(g m^{-3}) and E^t(g m^{-1} s^{-1}) are the concentration and the traffic-related emissions at a time "t", respectively. The linearity between C^t and E^t is defined by two parameters: C_0^t(g m^{-3}), which corresponds to the concentration level at the receptor location when emissions are from sources other than street traffic ($E^t = 0$), and D^t(s m^{-2}), which is a dilution factor that quantifies the dispersion resulting from turbulence induced either by atmosphere flows or vehicle

Fig. 1. Data collection site (Simon Bolivar Street). 1: Thermo-Scientific ADR 1500 profiler and traffic video recording. 2: AIRDAM anemometer. Adapted from Google Earth.

Table 1
Parameter settings used in OSPM model.

Parameters		Range	Interv.Step
Vehicle flux	total number of vehicles	0-2000 veh h^{-1}	200 veh h^{-1}
	% light-duty vehicles	0-100%	10%
Wind flows	wind speed	0–6.3 m s^{-1}	0.8 m s^{-1}
	wind direction	0-359°	15°

movements.

The traffic-related emission is a summation of all contributions of individual vehicle activities. Considering vehicles in a specific category "*i*" (e.g., light vehicles, motorcycles, heavy vehicles), traffic-related emission results in the following:

$$E^t = \sum_i N_i^t e_i \tag{2}$$

where E_i^t are the emissions released by the vehicles of category "*i*" at time "*t*";

N_i^t is the flux of vehicles belonging to category "*i*" in (veh-km h^{-1}); and
e_i is the emission factor of the vehicles of category "*i*" (in g km^{-1} veh^{-1}), which quantifies the amount of pollutant released by one vehicle travelling for 1-km.

Combining equations (1) and (2), we obtain the following:

$$C^t = \sum_i D^t N_i^t e_i + C_0^t \tag{3}$$

Assuming that e_i is constant with vehicle category, C^t and $D^t N_i^t$ data have to be multi-linearly related at each time "*t*". Note that N_i^t and C^t are measured data (i.e., vehicles fluxes and concentrations), while D^tdepends on elements that induce turbulence in the street canyon, such as meteorology or vehicle movements, and these elements can be measured (see section 3.2). Only $e_i$and C_0^t remain as unknown values.

3.2. Dilution factor

Previous studies have used predictions in wind tunnel simulations (Bruce et al., 2005; Huang et al., 2016) or have relied on gaseous tracers (Belalcazar et al., 2009; Zhang et al., 2015) as a measure of pollutant dilution. Our approach calculates exhaust emission dilution rates through modelling. Indeed, a plethora of dispersion models specially developed for, or simply used in, street canyon applications are available. There are no clear-cut distinctions between different categories, and models might be classified into groups according to their physical or mathematical principles (e.g., reduced-scale, box, Gaussian, CFD) and their level of complexity (e.g., screening, semi-empirical, numerical) (Vardoulakis et al., 2003). Accurate predictions are, in most cases, a function of meteorology, street geometry, receptor location and traffic volume.

In this work, we used the semi-empirical Operational Street Pollution Model—OSPM (Berkowicz and Danmark, 1997). The model choice was selected based on several aspects: it is robust and fast, contains all the essential parameters and dependencies observed in field data, and has been extensively validated for various street canyon types (Kakosimos et al., 2010). In addition, it has been previously used for similar purposes (e.g., Ketzel et al., 2003; Klose et al., 2009; Shunxi and Johansson n.d.). Concentrations of exhaust gases are calculated using a combination of a plume model for the direct impact of vehicle-emitted pollutants and a box model that enables computation of the additional impacts due to pollutants recirculated within the street by the vortex flow. For more details on the physical principles behind the modelling concept, the reader is referred to the original papers, e.g., Berkowicz 2000, Berkowicz et al., 1997, and Kakosimos et al., 2010.

According to Klose et al. (2009), pollutant dilution can be effectively simulated as a function of the turbulence induced by large-scale wind and vehicle motion. Parameters, such as fleet composition, street geometry, temperature and roof-level wind speed and direction, need to be defined implicitly for computing traffic-related emissions and concentrations. We performed simulations that use the experimental street canyon geometry and the in situ receptor location. Data provided by traffic counting (i.e., the composition and flux of vehicles) and by roof-level wind measurements were summarized, and their ranges were split into intervals (see Table 1). Then, for every possible combination of step-values for the percent of light-duty vehicles, as well as wind speed and direction, the slope of the linear regression plot of emissions vs. concentrations (i.e., resulting from the varying total number of vehicles) were presented as the corresponding dilution factor (rf. equation (1)). Note that fleet composition settings differentiate only light- and heavy-duty categories; an increase in the percent of light-duty vehicles (i.e., motorcycles, modern and old cars) forces the fraction of heavy-duty vehicles to decrease proportionally.

A three-dimensional array of wind speed (ws), wind direction (wd) and proportion of light-duty vehicles (α_i) is provided, and then we estimate dilution factors as a function of these parameters:

$$D = f(\alpha_i, wd, ws) \tag{4}$$

Hence, a dilution factor could be easily interpolated if turbulence is induced by parameters within the ranges shown in Table 1.

3.3. Time averaging

The literature suggests a wide spectrum of averaging times, e.g., −5, 15, 30 or 60 min (Belalcazar et al., 2009; Klose et al., 2009; Rey deCastro et al., 2008; Shunxi and Johansson n.d.), to assess the relationship between the raw data of pollutant emissions and concentrations. Most time frames reflect the temporal resolution of the data, but in reality, phenomena of chemical and mainly physical origins within the canyon could influence them.

In this study, we utilized data sampled at one-minute intervals. Based on equation (3), we aim to identify an averaging time that best relates "C^t" and "$D^t N_i^t$" data to maximize the robustness of the emission factor "e_i" estimations. Over a given time frame, emissions and concentrations are averaged as follows:

$$<C^t> = \frac{1}{n_t} \sum_{t=1}^{n_t} C^t \tag{5}$$

$$<E^t> = \sum_i \left[\frac{1}{n_t} \sum_{t=1}^{n_t} (D^t N_i^t) \cdot e_i \right] = \sum_i <D^t N_i^t> \cdot e_i \tag{6}$$

where n_t is the number of one-minute steps involved in computing the average.

Combining equations (5) and (6), we generalize the multilinear relationship between emissions and concentrations (rf. equation (3)):

$$<C^t> = \sum_i <D^t N_i^t> \cdot e_i + C_0 \tag{7}$$

Then, e_i can be approximated using the coefficients of the multiple linear regression (MLR) between $<C^t>$ and $<D^t N_i^t>$ data.

C_0 is interpreted as the intercept of the linear fit, so it is expected to be constant over the averaging time. Considering that it is a statistical value that characterizes the concentration measured at the receptor location when there is no street traffic, i.e., a background on the bottom, it likely varies with the temporal variation of external contributions. Nevertheless, their variability is expected -and therefore assumed-not to be statistically significant compared to the pollutant contributions of vehicles on the street.

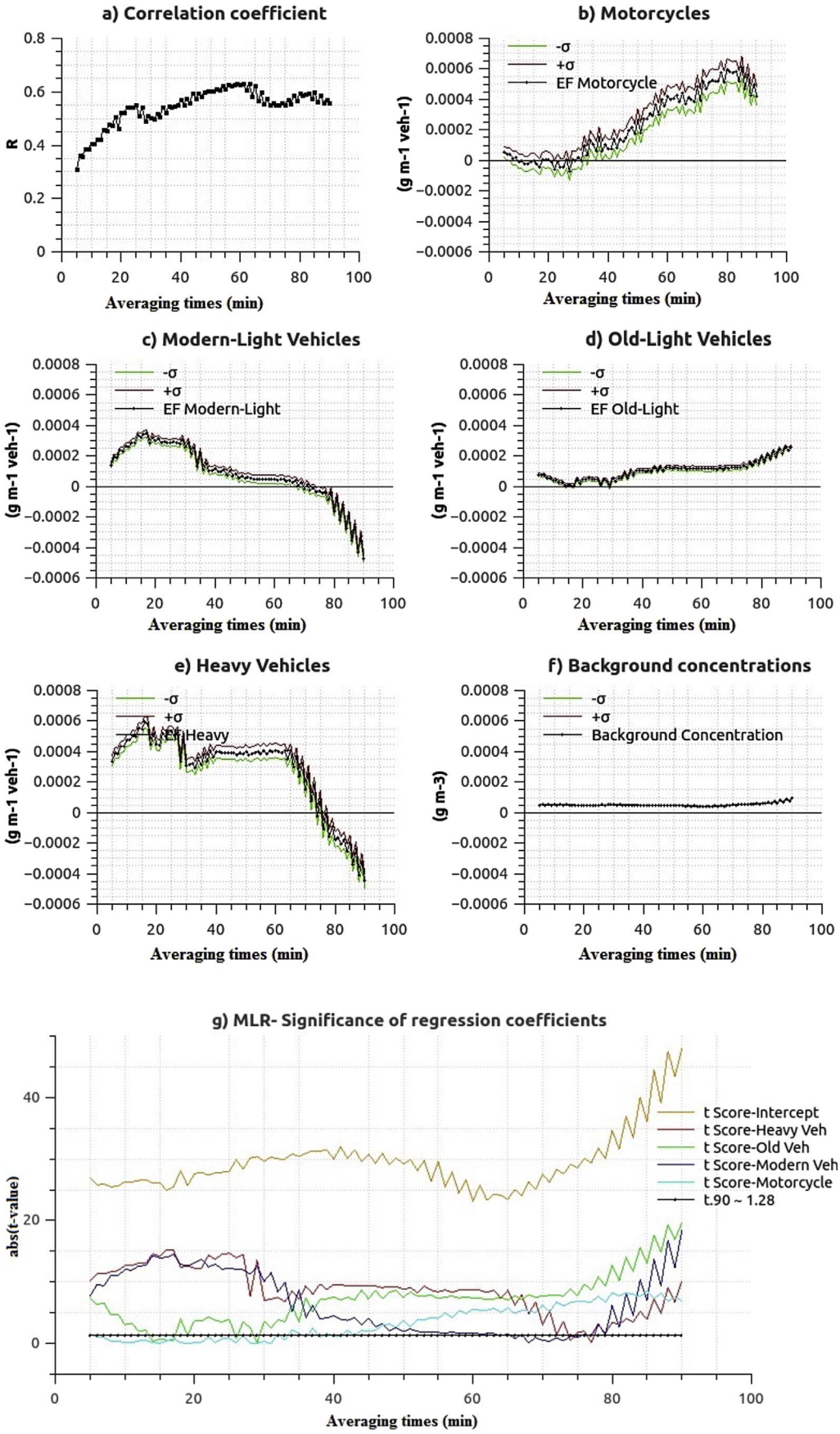

Fig. 2. Results of the multiple regression for different averaging times. (a) Correlation coefficient. (b–e) EF refers the coefficients of the regression or PM_{10} emission factors, and ± σ is the standard deviation of the coefficients. (f) The intercept and ± σ is the standard deviation of the intercept. (g) Significance levels of the regression coefficients.

4. Results and discussion

The methodology described in the previous section was implemented to estimate PM_{10} EFs of the vehicle fleet in Havana. Different averaging times, "n_t ", ranging from 5′ to 90′, were tested.

The quality of the regression fit is assessed by two criteria:

(i) the global correlation coefficient, "R", which is a measure of how well the EFs can be predicted using the MLR model from equation (7). The closer this value is to 1, the better the multilinear fit is.
(ii) The standard deviation, "σ", of each estimate, which measures how precisely the model estimates the unknown coefficient value. The smaller these values, the more precise the regression estimates (e_i-coefficients and C_0-intercept).

4.1. Multiple linear regression

Fig. 2a shows the correlation coefficient "R" at different averaging times, which range from 5′ to 90′. In Fig. 2b–f, the black points denote the coefficients (e_i- PM_{10} EFs in g m^{-1} veh^{-1} by vehicle category) and the intercept (C_0 - PM_{10} in g m^{-3}) from the MLR model. The red and green lines follow the standard deviations "σ" of these estimates.

The correlation coefficients were statistically significant for all averaging times (p-values < 6e-06). The best linear fits, i.e., the highest "R" values, were reached at approximately 60′. Overall, the MLR effectively estimates EFs for modern and old light-duty categories with greater precision, i.e., smaller "σ" values, than that for motorcycles and heavy vehicles. However, EFs are estimated with similar precision ("σ") by vehicle category, regardless of the averaging time length. To date, we are not able to indicate the specific averaging time that provides the best fit.

An overview of the extent of variability for all estimates over the tested averaging times can be seen in Table 2: the first row shows the average of the estimates. The standard deviation with respect to this mean (second row) concerns the variability regarding different averaging time lengths. The average of the standard deviations of the estimates (third row) refers to how spread out the set of estimates is across all averaging times. In summation, the square root of the sum of squared standard deviations (i.e., both the standard deviation of the estimates with respect to the mean and the average of the standard deviations of the estimates) describe how much the estimations vary. The variability caused by changes in averaging times is very high, even greater than the average of the individual standard deviations. Consequently, the total standard deviation (fourth row) associated with each EF is greater than the average EF itself.

Obviously, not all averaging times offer proper fits, and therefore, it is wrong to consider the entire set. Indeed, we realized that for averaging times < 40′ and > 60′, the t-value magnitudes of some coefficients are too small (< $t_{.90\sim1.28}$ in Fig. 2g) to declare them statistically significant. In between 40′ and 60′, we found a combination of good fits with estimates less impacted by the averaging time period used; the average standard deviation of the estimates (second row) in this time window decreases. Yet, it is lower than the average of the individual standard deviations (third row) for most of the vehicle categories (i.e., "modern light", "old light", and "heavy").

The high extent of variability in the motorcycle estimations is probably due to collinearity effects; in MLR models, when predictor variables are naturally correlated with each other -this refers to the presence of linear relationships between variables-a high global correlation coefficient "R" could indicate that predictions are correct but lead to a deceptive fit.

The correlation of predictors helps diagnose the existence of collinearity (Chennamaneni et al., 2016). For example, Table 4 shows the correlation matrix of predictors (i.e., parameters $<D^t N_i^t>$ in equation (7)) for an averaging time of 50'. Data for the "motorcycle", "modern light" and "old light" categories are highly positively correlated among themselves (Pearson correlation > 0.8), which indicates that, as the fluxes of vehicles belonging to one of these categories increase, the others also increase. The fluxes of "heavy" appear to be less related; this makes sense since this specific category mainly comprises buses that dominate the city's form of public transportation. Very similar correlation matrixes are found for another averaging time in the range of 40′-60′.

Table 2
Summary of multiple linear regressions – MLR; results (in mg km^{-1} veh^{-1}) for averaging times 5′-90'. Avg. EF: an average of coefficients for an emission factors; Std. Dev of the Avg. EF: the standard deviation of coefficients with respect to the mean; Avg. of the EFs Std. Dev: the average of the standard deviations of the coefficients. Total Std. Dev: summation of the square root of the sum of squared standard deviations; Std. Dev of the Avg. EF and Avg. of the EF's Std. Dev.

MLR (5′-90′)					
	Motorcycle	Modern-light veh	Old-light veh	Heavy veh	Backg. conc.
Avg. EF	231.2	85.6	103.5	282.5	51.4
Std. Dev of the Avg. EF	272.4	190.5	107.6	350.3	50.6
Avg. of the EF's Std. Dev	64.3	25.6	14.3	43.7	1.7
Total Std. Dev	279.9	192.2	108.5	353.0	50.6

Table 3
Summary of the multiple linear regression–MLR; results (in mg km^{-1} veh^{-1}) for averaging times 40′-60′. Avg. EF: an average of the coefficients for an emission factor; Std. Dev of the Avg. EF: the standard deviation of the coefficients with respect to the mean; Avg. of the EF's Std. Dev: the average of the standard deviations of the coefficients; Total Std. Dev: summation of the square root of the sum of squared standard deviations; Std. Dev of the Avg. EF and Avg. of the EF's Std. Dev.

MLR (40′-60′)					
	Motorcycle	Modern-light veh	Old-light veh	Heavy veh	Backg. conc.
Avg. EF	236.0	65.8	115.6	393.7	45.3
Std. Dev of the Avg. EF	100.6	21.4	8.6	8.6	2.2
Avg. of the EF's Std. Dev	69.1	26.6	15.0	44.0	1.6
Total Std. Dev	122.0	34.1	17.3	44.8	2.7

4.2. Principal component regression

Principal component regression (PCR) succeeds in overcoming the collinearity problem that arises when two or more predictor variables are correlated. Based on a principal component analysis (PCA), this procedure converts the set of correlated predictors into a set of linearly uncorrelated variables called principal components (the number of principal components is equal to the number of original predictors). By excluding some of the low-variance principal components in the regression step, the PCR can aptly estimate the regression coefficients that characterize the original model.

When we retain the three principal components with the highest variances, i.e., sufficient to explain 90% of the variance of the original

Table 4
Correlations matrix of predictor variables for a time period of 50′.

Correlation matrix	Motorcycle	Modern-light veh	Old-light veh	Heavy veh
Motorcycle	1.00	0.85	0.86	0.58
Modern-Light veh	0.85	1.00	0.84	0.49
Old-Light veh	0.86	0.84	1.00	0.60
Heavy veh	0.58	0.49	0.60	1.00

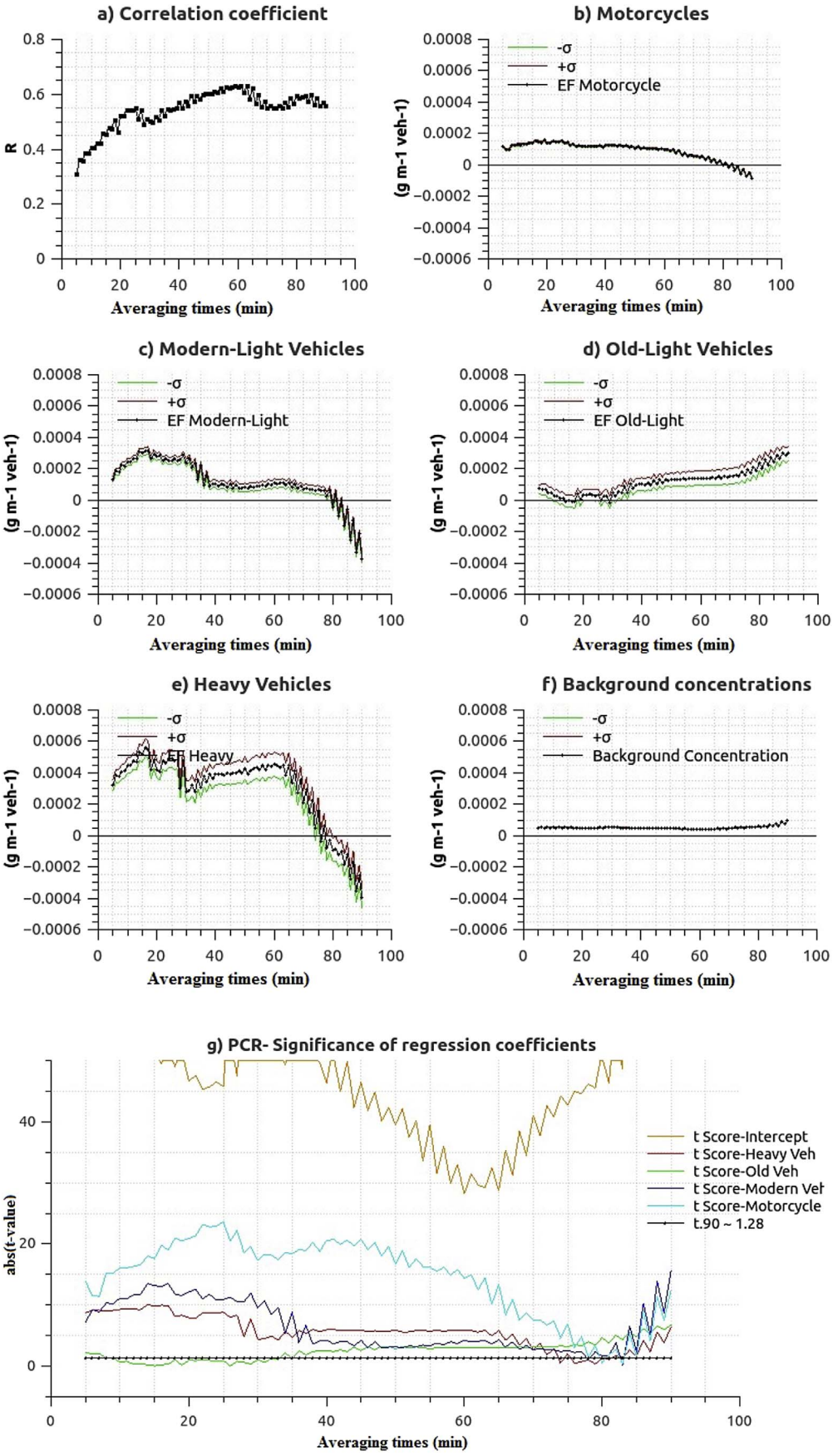

Fig. 3. Results of the principal component regression for different averaging time periods. (a) Correlation coefficient. (b–e) EF is the PM_{10} emission factor, i.e., the coefficients of the regression; ± σ is the standard deviation of the coefficients. (f) Background concentrations: the intercept ± σ is the standard deviation of the intercept.

Table 5
Summary of the principal component regression (PCR) results (in mg km^{-1} veh^{-1}) for averaging times 40′-60′. Avg. EF: the average of the coefficients for an emission factor; Std. Dev of the Avg. EF: the standard deviation of the coefficients with respect to the mean; Avg. of the EF's Std. Dev: the average of the standard deviations of the coefficients; Total Std. Dev: summation of the square root of the sum of squared standard deviations; Std. Dev of the Avg. EF and Avg. of the EF's Std. Dev.

PCR (40′-60′)					
	Motorcycle	Modern-light veh	Old-light veh	Heavy veh	Backg. conc.
Avg. EF	111.1	90.6	125.4	415.1	44.3
Std. Dev of the Avg. EF	9.5	10.6	14.6	22.3	3.0
Avg. of the EF's Std. Dev	6.2	25.5	42.8	71.5	1.1
Total Std. Dev	11.3	27.6	45.2	74.9	3.2

predictor variables, all correlation coefficients remain significant (p-values < 6e-06). Although Fig. 3a shows that "R" is slightly lower based on the PCR than based on the MLR (indicating lower quality in the fits), there is an observed improvement in the estimates of motorcycle EFs (black line in Fig. 3b), which is almost unaffected by the averaging time lengths. The t-values of all coefficients remain statistically significant between 40′-60′ with a 90% probability (see Fig. 3g). In Table 5, we summarize the new estimates and their extent of variability. We use and recommend the PCR method since it represents a good compromise between fitting quality and estimate accuracy.

4.3. Considering uncertainties in EF estimations

In Table 5, the total standard deviation may be primarily due to three assumptions inherent in this methodology: (i) the EFs are constant in each vehicle category; (ii) the background concentration at the receptor location is constant over the averaging time; and (iii) the variability of the dilution factor depends exclusively on the variation of the proportion of light-duty vehicles, wind speed and wind direction.

To capture the uncertainties inherent in such assumptions, we consider the average EFs and total standard deviations, "δ", from the PCR for 40′-60′ using a normal distribution function. The function used to describe the normal distribution is symmetric and valid for pre-defined boundaries of contiguous values (Alamilla-López, 2015). We generate a sequence of values from $(EF - 3\delta)$ to $(EF + 3\delta)$ and calculate a probability density function (PDF) for each vehicle category (see Fig. 4), thereby producing justified estimates of the uncertainties for EFs. Within the boundaries of the 95% confidence interval of the PDF, the EFs are probably within the range bounded by $\overline{EF} \pm Z\frac{\delta^2}{\sqrt{n}}$, where $z = 1.96$ for $\alpha = 0.05$. Thus, motorcycles have an EF = 111.1 ± 2.7 mg km^{-1} veh^{-1}; modern, light vehicles have an EF = 90.6 ± 11.2 mg km^{-1} veh^{-1}; old, light vehicles have an EF = 125.4 ± 18.5 mg km^{-1} veh^{-1}; and heavy vehicles have an EF = 415.1 ± 31.2 mg km^{-1} veh^{-1}. The bounded values are given in absolute terms, and they characterize the range of values within which the EFs of the different categories are assumed to be in, based on the specified level of confidence. They illustrate the scatter in data due to the statistical assumptions made in the linear fitting, but they also consider that the EFs of vehicles in a single category could provide different results due to unavoidable variation in the amount of pollutants that vehicles are emitting. The bounded values refer all contributing uncertainties, including those generated by the assumptions mentioned in the previous paragraph, while the PDFs allow for inferring the probability of finding a vehicle that pollutes more or less within a single category.

4.4. Comparisons with available studies

Regional differences are commonly expected in vehicle EFs for several reasons, including local applications of emission regulations, local driver behaviours or the quality of the fuel in use.

From a literature review conducted by Bond et al. (2004), the average emission rate for light-duty gasoline and diesel is 21.0 ± 14.0 mg km^{-1} veh^{-1} (for unit conversions, we assumed average fuel consumption of 0.2 L km^{-1}) in regions where emission standards have been progressively tightened; pre-1985 cars had average emission rates of approximately 33.6 mg km^{-1} veh^{-1}. For other regions, an average of 70.0 ± 56.0 mg km^{-1} veh^{-1} was used, which is still lower than the values obtained in our study. Yan et al. (2011) relied on measurements from previous studies (Ntziachristos, 2001; Ubanwa et al., 2003; Yanowitz et al., 2000) for vehicles built without standards; they applied values of 7 and 250 mg km^{-1} veh^{-1} for light-duty gasoline and diesel vehicles, respectively. Such a large range encompasses our calculated EFs for light-duty vehicles (i.e., modern and old categories).

Ntziachristos et al. (2012) reported motorcycle PM_{10} EFs that comply with European emission standards (i.e., Euro I, Euro II, etc.); the average result was 34 mg km^{-1} veh^{-1}. For uncontrolled motorcycle technologies, the value of 77 mg km^{-1} veh^{-1} was used. These emission rates are lower than the estimates in the present study.

From a review of in-use heavy-duty diesel EFs, made by Yanowitz et al. (2000), the average from more than 250 different vehicles reported in 20 worldwide studies was 845.0 ± 56.0 mg km^{-1} veh^{-1}. For 2008, the value reported by the U.S. EPA (2008) for in-use heavy-duty gasoline vehicles was 316.9 mg km^{-1} veh^{-1}. In Yan et al. (2011),

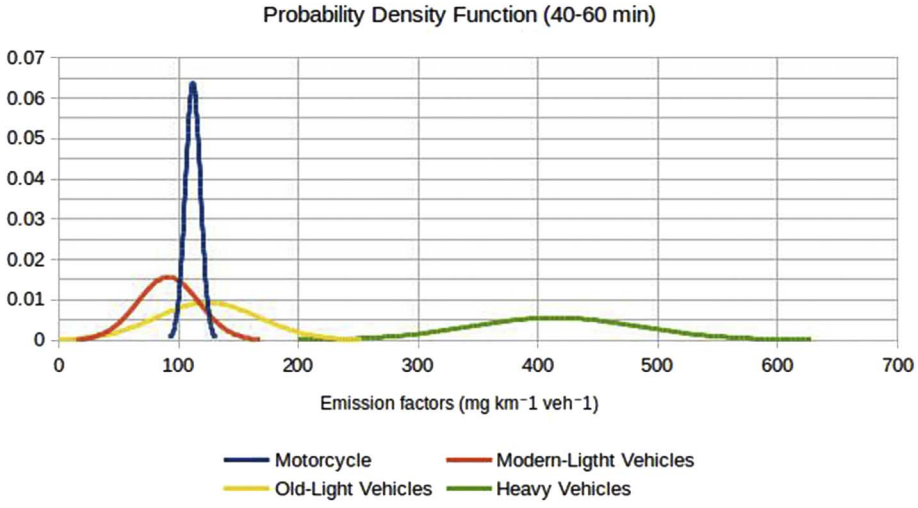

Fig. 4. Probability density functions. The curves express the range of variation of PM_{10} EFs (mg km^{-1} veh^{-1}) by vehicle category.

Table 6
Estimated traffic emission factors (mg km^{-1} veh^{-1}) for 33.3% vehicle fractions from the PDFs.

Vehicle categories		EFs
Motorcycle	low-polluting	105.1
	medium-polluting	111.8
	high-polluting	118.5
Modern-light veh	low-polluting	63.7
	medium-polluting	91.3
	high-polluting	118.9
Old-light veh	low-polluting	78.4
	medium-polluting	124.2
	high-polluting	170.5
Heavy veh	low-polluting	336.6
	medium-polluting	413.8
	high-polluting	491.0

the proposed average values for heavy-duty vehicles built with and without standards were 280 and 700 mg km^{-1} veh^{-1}, respectively. Considering that we included diesel and gasoline heavy-duty vehicles in a single category, our estimation aligns with the reference literature.

The fraction of vehicles using the poorest technologies or having the worst maintenance are commonly classified as high-polluting or "super-emitters" (Bond et al., 2004; McCormick et al., 2003; Subramanian et al., 2009; Yan et al., 2011) and contribute significantly to total emissions (Hansen and Rosen, 1990; Lawson, 1993; Zhang et al., 1995). The division between super-emitters and normal emitters affects the assumed emission factor for each technology category (Yan et al., 2014). For gasoline vehicles, Bond et al. (2004) reported a super-emitter EF of approximately 280 mg km^{-1} veh^{-1}; the average value reported by Durbin et al. (1999) and Cadle et al. (1999) was approximately 250 mg km^{-1} veh^{-1}. For diesel vehicles, in Bond et al. (2004), the average of super-emitters was more than 2 g km^{-1} veh^{-1}, which is in agreement with studies by McCormick et al. (2003) and Subramanian et al. (2009). The PDFs in section 4.3 allow us to identify high-polluting vehicles within a single category. We computed the most likely EFs bred from a desired area under the PDFs. In Table 6, we distinguish three sub-categories by breaking each category into one-third increments (i.e., fractions of 33.3% of vehicles in each sub-category) of the PDF surfaces. According to this fragmentation, we estimate that high-polluting motorcycles and modern-light vehicles have EF values of approximately 118.5 mg km^{-1} veh^{-1}. For the old-light and heavy categories, the EF values are 170.5 and 491.0 mg km^{-1} veh^{-1}.

5. EFs for air pollution policy purposes

In this section, we explore the potential of different traffic-related scenarios for the abatement of PM_{10} air pollution. The scenarios highlight changes in emission factors, e_i, and help assess the expected PM_{10} reductions that could be achieved by upgrading, renewing or restricting the vehicle fleet in Havana. First, we define a reference situation that states the diurnal hourly PM_{10} concentration levels by considering the following:

- The background concentration at the receptor location C_0 obtained from PCR (section 4.2, Table 5).
- The emission factors, e_i, classified into sub-categories; these are based on the PCR results in section 4.2 and the PDFs described in section 4.3, Table 6.
- A constant vehicle flux by category, $<N_i^t> = N_i$, which is equal to the average of the measurements provided by traffic counting.
- The induced turbulence through four diurnal periods *"P"*. Dilution factors $<D^t>^P$ are estimated considering minimal variation by period (period 1 = 7:00–9:00; period 2 = 9:00–12:00, period 3 = 12:00–13:00 & 16h00-19h00 period 4 = 13h00-16h00).

Table 7
Estimated PM_{10} hourly diurnal concentration levels (μg m^{-3}).

Vehicle categories		Hourly diurnal concentration (μg m^{-3})
Motorcycles	low-polluting	1.4
	medium-polluting	1.5
	high-polluting	1.5
Modern-Light veh	low-polluting	2.2
	medium-polluting	3.2
	high-polluting	4.2
Old-Light veh	low-polluting	5.6
	medium-polluting	8.9
	high-polluting	12.2
Heavy veh	low-polluting	4.0
	medium-polluting	5.0
	high-polluting	5.9
Traffic		**55.5 (*56%*)**
Background		**44.3 (*44%*)**
Total		**99.8**

Bold: contributions to PM10 air pollution (amounts from traffic and other sources -background) in the street canyon.
Bold and Italic: percent of contributions to PM10 air pollution (from traffic and other sources -background) in the street canyon with respect to the total amount.

Referring to all these, equation (7) can be written as follows:

$$<C^t>^P = \sum_i <D^t>^P \cdot N_i \cdot e_i + C_0 \quad (8)$$

It considers the contributions of all sources in the street (see Table 7). Traffic sources are responsible for approximately 56% of PM_{10} air pollution. The largest contributors are old-light and heavy vehicles, in that order. Other sources may include the Havana Refinery and the Thermoelectric, which both have constant operating regimens within a 5-km radius from the measurement site, as well as traffic on surrounding streets.

Thereafter, we forecast the effects of progressive technological improvements (see Fig. 5). Starting from the largest contributor categories, the first scenario imagines the upgrading of old-light vehicles by reducing their EFs to 78.4 mg km^{-1} veh^{-1} (i.e., the EF of low-polluting, old-light vehicles). The second scenario considers a total renewal of this category by reducing their EFs to 63.7 mg km^{-1} veh^{-1} (i.e., the EF of low-polluting, modern-light vehicles). In the third scenario, we assume that all light vehicles belong to the modern, low-polluting category. The last scenario adds the upgrading of heavy vehicles by setting the EFs of medium and high polluting vehicles to 336.6 mg km^{-1} veh^{-1} (i.e., the EF of low-polluting, heavy vehicles). Fig. 5 shows the abatements of two percentages: one with respect to the traffic contributions on the street (red arrows), and the other considers the background concentrations (black arrows). The upgrading of vehicles in the old-light category (scenario 1) seems to be the most effective scenario. Alone, this scenario attains half of the PM_{10} abatement that could be achieved with all cumulative improvements (scenario 4).

If these improvements are implemented across Havana, the background concentrations on any given street would decrease as a result of the reduction of external traffic sources. Then, the percent of reduction with respect to traffic on each street (red arrows) could be greater than the values calculated. Hence, the values indicate the minimum expected abatement for each scenario. Conversely, by adding all possible reductions from sources other than traffic, the corresponding percentage with respect to the contributions on the street (black arrows) indicates the maximum expected abatement for each scenario. These percentages give an idea of the global scope expected (in percent) based on our different technological scenarios.

Greater abatement could be obtained by adding traffic restrictions. This can be seen in Fig. 6, which shows the effects of replacing the light-duty traffic, motorcycles and trucks (in that order) with low-polluting buses with 120-passenger capacities (See Table 8). This implies an increase in the number of buses for passengers to travel on.

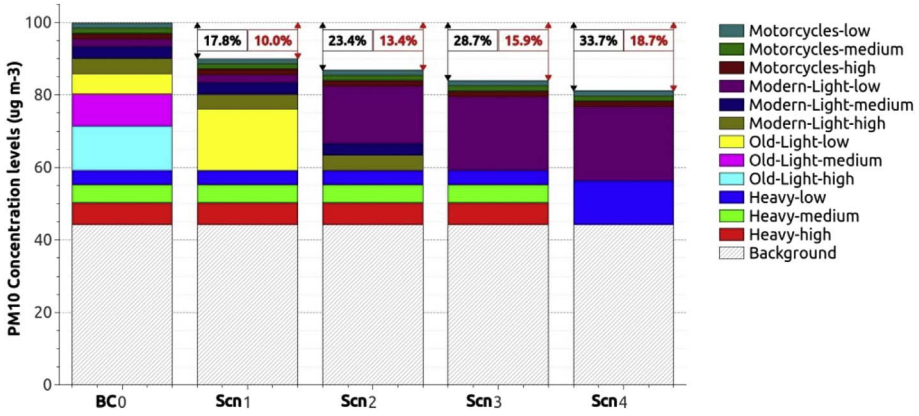

Fig. 5. Comparison of PM_{10} concentration levels (μg m^{-3}) from on-road vehicles under four scenarios. Red and black arrows indicate the minimum and maximum percent of reduction expected on the street.

The black-dotted line represents the evolution of the baseline case. A maximum reduction of 35.5 μg m^{-3} (from 55.5 to 20.0 μg m^{-3}) is expected by restricting the circulation of all light vehicles. Approximately 4 and 5 μg m^{-3} of PM_{10} would be reduced by restricting motorcycles and trucks, respectively. Such situations easily decrease the street PM_{10} air pollution. For the blue and red dashed lines, we combine the same traffic restrictions with some technological improvements; these consider that all light vehicles exclusively belong to the modern- or old-light categories, respectively. Therefore, these lines (black-dotted, red and blue dashed) could be useful for developing strategies to reduce pollutants. For example, when examining the reduction to 40 μg m^{-3} from the "baseline case" (i.e., the start of the black-dotted line), the reduction can be attained either by upgrading light vehicles to modern categories (passing to the blue-dashed line) or by restricting their circulation (moving onto the black-dotted line) to 560 veh h^{-1}, which would require approximately 80% of passengers to travel by bus.

The grey lines add the effects of upgrading light vehicles to modern ones while decreasing the average number of vehicle passengers. In terms of travel comfort, this is a likely future situation that can be considered in Havana; it implies an overall increase in the use of modern vehicles for moving passengers. For example, if the number of passengers is reduced to two and they travel in a modern-light vehicle

Table 8
Passenger transport capacity used for projections.

Vehicle category	Average passenger (η)
Motorcycles	2
Modern-light veh	4
Old-light veh	5
Buses	120
Trucks	1

(η = 2), an increase of 10 μg m^{-3} (from 55.5 to 65.4 μg m^{-3}) would be expected compared to the "baseline case".

Fig. 6 also shows the minimum and maximum percentages (axes at right) of reduction that could be expected in the entire city by implementing any of the strategies displayed in the graphs.

6. Conclusions

In this study, we established a methodology to estimate traffic emission factors from street canyon measurements (low-cost devices) of traffic fluxes, wind forces and concentration levels, and all data were collected in one-minute time steps. The methodology was based on the

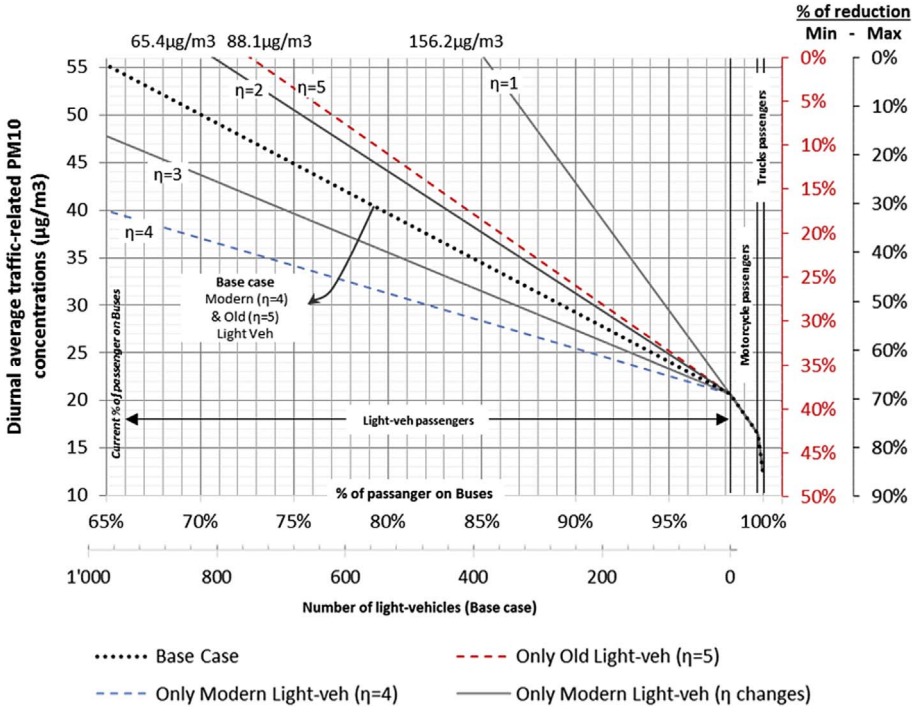

Fig. 6. Projection lines of PM_{10} concentration levels based on reductions from 55 to 10 (μg m-3), as expected from decreasing the number of light-duty vehicles from 1000 to 0 along with an increase in passengers that travel on buses from 65 to 100% and/or changing light-duty vehicle capacities. (See Table 3). The percentages on the right (red and black) indicate the minimum and maximum reductions expected on the street.

assumption that inside the street canyon and over a given time period, the average traffic emissions are linearly related to the average concentrations of slowly reactive pollutants. Thus, under well-defined wind forces and traffic conditions, a dilution factor was calculated, and multilinear regression techniques were used for estimating an average emission factor for each vehicle category.

The implementation of principal component regressions is preferred over standard multiple regression techniques since it reduces the collinearity effects that appear when traffic fluxes are naturally correlated between vehicle categories. The application of PM_{10} EFs on the four vehicle categories in Havana's fleet showed the best regression fits ($R > 0.5$ and standard deviation of estimates < 15%) when averaging the data between 40′ and 60’.

It was found that traffic sources are responsible for over 50% of PM_{10} air pollution on the street; among all vehicles, the largest contributors are old, light-duty vehicles. A coarse forecasting indicated that upgrading this category (i.e., a decrease of EF to 78 mg km^{-1}) would be an effective scenario for reducing PM_{10} air pollution in Havana by between 10 and 17%.

The next steps include improving dilution factor estimations by generalizing; for example, the effects of street geometry and receptor location could be considered. The method is expected to be extended and validated for other pollutants in order to develop sound policies for the control and management of traffic-related pollution in the city of Havana.

Acknowledgements

The authors of this study thank the Swiss National Science Foundation (SNF Grant Number 160914) for the funding provided to this project. We would also like to thank the research team of the Centro de Contaminación y Quimica Atmosférica (CECONT) of the National Institute of Meteorology in Cuba for providing us support with obtaining data. We especially thank Prof François Golay and Prof François Marechal from Ecole Polytechnique Fédéral de Lausanne for their invaluable support in carrying out this project.

References

Ait-Helal, W., et al., 2015. On-road measurements of NMVOCs and NO X: determination of light-duty vehicles emission factors from tunnel studies in Brussels city center. Atmos. Environ. 122, 799–807. Retrieved August 17, 2017. http://linkinghub.elsevier.com/retrieve/pii/S1352231015304088.

Alamilla-López, Jorge Luis, 2015. An approximation to the probability normal distribution and its inverse. Ing. Investig. Tecnol. 16 (4), 605–611. Retrieved September 7, 2017. http://linkinghub.elsevier.com/retrieve/pii/S1405774315000451.

Amato, F., et al., 2016. Traffic induced particle resuspension in Paris: emission factors and source contributions. Atmos. Environ. 129, 114–124. Retrieved August 17, 2017. http://linkinghub.elsevier.com/retrieve/pii/S1352231016300309.

Belalcazar, Carlos, Luis, Clappier, Alain, Blond, Nadège, Flassak, Thomas, Eichhorn, Joachim, 2010. An evaluation of the estimation of road traffic emission factors from tracer studies. Atmos. Environ. 44 (31), 3814–3822. Retrieved October 28, 2012. http://linkinghub.elsevier.com/retrieve/pii/S1352231010005170.

Belalcazar, Carlos, Luis, Fuhrer, Oliver, Dung Ho, Minh, Zarate, Erika, Clappier, Alain, 2009. Estimation of road traffic emission factors from a long term tracer study. Atmos. Environ. 43 (36), 5830–5837. Retrieved October 28, 2012. http://linkinghub.elsevier.com/retrieve/pii/S1352231009006712.

Berkowicz, Ruwim, 2000. OSPM - a parameterised street pollution model. Environ. Monit. Assess. 65, 323–331. Retrieved. http://www.springerlink.com/index/QL86805806122454.pdf.

Berkowicz, Ruwim, Danmark, Miljøundersøgelser, 1997. Modelling Traffic Pollution in Streets. Ministry of Environment and Energy, National Environmental Research Institute.

Berkowicz, Ruwim, Hertel, Ole, Larsen, Se, Sørensen, Nn, Nielsen, M., 1997. Modelling traffic pollution in streets. Natl. Environ. Res. Inst. Roskilde Den. 10129 (10136), 20. http://www.mst.dk/NR/rdonlyres/9D313499-E237-4C1A-ADC4-D31737E31613/0/A11_ModellingTrafficPollutioninStreets.pdf.

Bond, Tami C., et al., 2004. A technology-based global inventory of black and organic carbon emissions from combustion. J. Geophys. Res. D Atmos. 109 (14), 1–43.

Borrego, C., et al., 2016. Urban scale air quality modelling using detailed traffic emissions estimates. Atmos. Environ. 131, 341–351.

Brimblecombe, Peter, et al., 2015. Through-tunnel estimates of vehicle fleet emission factors. Atmos. Environ. 123, 180–189. Retrieved August 17, 2017. http://linkinghub.elsevier.com/retrieve/pii/S1352231015305021.

Bruce, R., Coquilla, Rachael, Kuspa, Bethany, Padilla, Angelina, 2005. A Wind-tunnel Study of Air Re-entrainment from an Accidental Laboratory Exhaust Stack Release on the UC Davis Watershed Science Research Center.

Cadle, Steven H., et al., 1999. Composition of light-duty motor vehicle exhaust particulate matter in the denver, Colorado area. Environ. Sci. Technol. 33 (14), 2328–2339.

Chennamaneni, Pavan Rao, Echambadi, Raj, Hess, James D., Syam, Niladri, 2016. Diagnosing harmful collinearity in moderated regressions: a roadmap. Int. J. Res. Mark. 33 (1), 172–182. Retrieved August 30, 2017. http://linkinghub.elsevier.com/retrieve/pii/S0167811615001068.

Durbin, Thomas D., Smith, Matthew R., Norbeck, Joseph M., Truex, Timothy J., 1999. Population density, particulate emission characterization, and impact on the particulate inventory of smoking vehicles in the south coast air quality management district. J. Air Waste Manag. Assoc. 49 (1), 28–38. Retrieved. http://www.engineeringvillage.com/blog/document.url?mid=cpx_b753f811bff4dd3b0M75c12061377553&database=cpx%5Cnhttps://www.engineeringvillage.com/blog/document.url?mid=cpx_b753f811bff4dd3b0M75c12061377553&database=cpx.

EPA, (United States Enviromental Protection Agency/Office of Transportation and Air Quality), 2008. Average in-Use Emission for Heavy-duty Trucks. Retrieved. https://nepis.epa.gov/Exe/ZyNET.exe/P100EVY6.txt?ZyActionD=ZyDocument&Client=EPA&Index=2006 Thru 2010&Docs=&Query=&Time=&EndTime=&SearchMethod=1&TocRestrict=n&Toc=&TocEntry=&QField=&QFieldYear=&QFieldMonth=&QFieldDay=&UseQField=&IntQFieldOp=0&ExtQFieldOp=).

Ferm, Martin, Sjöberg, Karin, 2015. Concentrations and emission factors for PM 2.5 and PM 10 from road traffic in Sweden. Atmos. Environ. 119, 211–219. Retrieved August 17, 2017. http://linkinghub.elsevier.com/retrieve/pii/S135223101530282X.

Gertler, Alan W., Pierson, William R., Watson, John G., Bradow, Ronald L., 1991. Review and Reconciliation of on-Road Emission Factors in the South Coast Air Basin.

Hansen, A.D.A., Rosen, H., 1990. Individual measurements of the emission factor of aerosol black carbon in automobile plumes. J. Air Waste Manag. Assoc. 40 (12), 1654–1657.

Huang, Yuan-dong, Zengf, Ning-bin, Liu, Ze-yu, Song, Ye, Xu, Xuan, 2016. Wind tunnel simulation of pollutant dispersion inside street canyons with galleries and multi-level flat roofs. J. Hydrodyn. Ser. B 28 (5), 801–810. Retrieved September 4, 2017. http://linkinghub.elsevier.com/retrieve/pii/S1001605816606832.

Jaikumar, Rohit, Shiva Nagendra, S.M., Sivanandan, R., 2017. Modeling of real time exhaust emissions of passenger cars under heterogeneous traffic conditions. Atmos. Pollut. Res. 8 (1), 80–88. Retrieved August 31, 2017. http://linkinghub.elsevier.com/retrieve/pii/S1309104216300691.

Jung, Sungwoon, et al., 2017. Characterization of particulate matter from diesel passenger cars tested on chassis dynamometers. J. Environ. Sci. 54, 21–32. Retrieved August 17, 2017. http://linkinghub.elsevier.com/retrieve/pii/S1001074216301954.

Kakosimos, Konstantinos E., Hertel, Ole, Ketzel, Matthias, Berkowicz, Ruwim, 2010. Operational street pollution model (OSPM) - a review of performed application and validation studies, and future prospects. Environ. Chem. 7 (6), 485–503.

Kam, Winnie, Liacos, James W., Schauer, James J., Delfino, Ralph J., Sioutas, Constantinos, 2012. On-road emission factors of PM pollutants for light-duty vehicles (LDVs) based on urban street driving conditions. Atmos. Environ. 61, 378–386. Retrieved August 17, 2017. http://linkinghub.elsevier.com/retrieve/pii/S1352231012007583.

Kastner-Klein, Petra, Fedorovich, Evgeni, Ketzel, Matthias, Berkowicz, Ruwim, Britter, Rex, 2003. The modelling of turbulence from traffic in urban dispersion models - Part II: evaluation against laboratory and full-scale concentration measurements in street canyons. Environ. Fluid Mech. 3 (2), 145–172.

Ketzel, Matthias, Berkowicz, Ruwim, Lohmeyer, Achim, 2000. Comparison of numerical street dispersion models with. Environ. Monit. Assess. 65 (1–2), 363–370. Retrieved. http://link.springer.com/article/10.1023%2FA%3A1006460724703.

Ketzel, Matthias, Wåhlin, Peter, Berkowicz, Ruwim, Palmgren, Finn, 2003. Particle and trace gas emission factors under urban driving conditions in copenhagen based on street and roof-level observations. Atmos. Environ. 37 (20), 2735–2749. Retrieved August 17, 2017. http://linkinghub.elsevier.com/retrieve/pii/S1352231003002450.

Keuken, M.P., et al., 2016. Particle number concentration near road traffic in amsterdam (The Netherlands): Comparison of standard and real-world emission factors. Atmos. Environ. 132, 345–355. Retrieved August 17, 2017. http://linkinghub.elsevier.com/retrieve/pii/S1352231016301807.

Klose, S., et al., 2009. Particle number emissions of motor traffic derived from street canyon measurements in a central European city. Atmos. Chem. Phys. Discuss. 9 (1), 3763–3809. Retrieved August 17, 2017. http://www.atmos-chem-phys-discuss.net/9/3763/2009/.

Lawson, Douglas R., 1993. ‘Passing the test:’ human behavior and California's smog check program. Air Waste December 1993 1567–1575.

Li, Tiezhu, Chen, Xudong, Yan, Zhenxing, 2013. Comparison of fine particles emissions of light-duty gasoline vehicles from chassis dynamometer tests and on-road measurements. Atmos. Environ. 68, 82–91. Retrieved August 17, 2017. http://linkinghub.elsevier.com/retrieve/pii/S135223101201093X.

McCormick, Robert L., Graboski, Michael S., Alleman, Teresa L., Alvarez, Javier R., Duleep, K.G., 2003. Quantifying the emission benefits of opacity testing and repair of heavy-duty diesel vehicles. Environ. Sci. Technol. 37 (3), 630–637.

Moradpour, Maryam, Afshin, Hossein, Farhanieh, Bijan, 2017. A numerical investigation of reactive air pollutant dispersion in urban street canyons with tree planting. Atmos. Pollut. Res. 8 (2), 253–266. Retrieved August 17, 2017. http://linkinghub.elsevier.com/retrieve/pii/S1309104216302471.

Nakashima, Yoshihiro, Kajii, Yoshizumi, 2017. Determination of nitrous acid emission factors from a gasoline vehicle using a chassis dynamometer combined with incoherent broadband cavity-enhanced absorption spectroscopy. Sci. Total Environ. 575, 287–293. Retrieved August 17, 2017. http://linkinghub.elsevier.com/retrieve/

pii/S0048969716322161.
Ntziachristos, L., 2001. An empirical method for predicting exhaust emissions of regulated pollutants from future vehicle technologies. Atmos. Environ. 35 (11), 1985–1999. Retrieved August 21, 2017. http://linkinghub.elsevier.com/retrieve/pii/S1352231000004714.
Ntziachristos, Leonidas, et al., 2012. EMEP/EEA Emission Inventory Guidebook 2009, Updated May 2012 1. (May).
Palmgren, Finn, Berkowicz, Ruwim, Ziv, Alexander, Hertel, Ole, 1999. Actual car fleet emissions estimated from urban air quality measurements and street pollution models. Sci. Total Environ. 235 (1–3), 101–109. Retrieved August 17, 2017. http://linkinghub.elsevier.com/retrieve/pii/S0048969799001965.
Pang, Yanbo, Fuentes, Mark, Rieger, Paul, 2014. Trends in the emissions of volatile organic compounds (VOCs) from light-duty gasoline vehicles tested on chassis dynamometers in southern California. Atmos. Environ. 83, 127–135. Retrieved August 17, 2017. http://linkinghub.elsevier.com/retrieve/pii/S1352231013008303.
Rey deCastro, B., et al., 2008. The longitudinal dependence of black carbon concentration on traffic volume in an urban environment. J. Air Waste Manag. Assoc. 58 (7), 928–939. Retrieved. http://secure.awma.org/onlinelibrary/doihandler.aspx?doicode=10.3155-1047-3289.58.7.928.
Riccio, A., et al., 2016. Real-world automotive particulate matter and PAH emission factors and profile concentrations: results from an urban tunnel experiment in naples, Italy. Atmos. Environ. 141, 379–387. Retrieved August 17, 2017. http://linkinghub.elsevier.com/retrieve/pii/S1352231016305118.
Shunxi Deng and Christer Johansson. n.d. "Traffic Emission Factors of Particle Number Measured in a Street Canyon in Stockholm, Sweden." Retrieved (https://www.dri.edu/images/stories/editors/leapfrog/techprog/IIe_4_Deng.pdf).
Smit, R., Kingston, P., Wainwright, D.H., Tooker, R., 2017. A tunnel study to validate motor vehicle emission prediction software in Australia. Atmos. Environ. 151, 188–199. Retrieved September 6, 2017. http://linkinghub.elsevier.com/retrieve/pii/S1352231016309736.
Sokhi, Ranjeet S., et al., 2008. An integrated multi-model approach for air quality assessment: development and evaluation of the OSCAR air quality assessment system. Environ. Model. Softw. 23 (3), 268–281. Retrieved May 14, 2015. http://linkinghub.elsevier.com/retrieve/pii/S1364815207000813.
Subramanian, R., et al., 2009. Climate-relevant properties of diesel particulate Emissions: results from a piggyback study in Bangkok, Thailand climate-relevant properties of diesel particulate Emissions: results from a piggyback study in Bangkok, Thailand. Environ. Sci. Technol. 43 (11), 4213–4218.
Ubanwa, B., Burnette, A., Kishan, S., Fritz, S.G., 2003. Exhaust particulate matter emission factors and deterioration rate for in-use. J. Eng. Gas Turbines Power 125 (April), 513–523.
Vardoulakis, Sotiris, Fisher, Bernard E., Pericleous, Koulis, Gonzalez-Flesca, Norbert, 2003. Modelling air quality in street canyons: a review. Atmos. Environ. 37 (2), 155–182. Retrieved August 17, 2017. http://linkinghub.elsevier.com/retrieve/pii/S1352231002008579.
Wang, Yuan, Huang, Zihan, Liu, Yujie, Yu, Qi, Ma, Weichun, 2017. Back-calculation of traffic-related PM10 emission factors based on roadside concentration measurements. Atmosphere 8 (6), 99. Retrieved. http://www.mdpi.com/2073-4433/8/6/99.
Yan, Fang, Winijkul, Ekbordin, Bond, Tami C., Streets, David G., 2014. Global emission projections of particulate matter (PM): II. Uncertainty analyses of on-road vehicle exhaust emissions. Atmos. Environ. 87, 189–199. Retrieved August 17, 2017. http://linkinghub.elsevier.com/retrieve/pii/S1352231014000703.
Yan, Fang, Winijkul, Ekbordin, Jung, Soonkyu, Bond, Tami C., Streets, David G., 2011. Global emission projections of particulate matter (PM): I. Exhaust emissions from on-road vehicles. Atmos. Environ. 45 (28), 4830–4844. Retrieved August 17, 2017. http://linkinghub.elsevier.com/retrieve/pii/S135223101100611X.
Yanowitz, Janet, Mccormick, Robert L., Graboski, Michael S., 2000. "In-Use emissions from heavy-duty diesel vehicles. Environ. Sci. Technol. 34 (5), 729–740. http://dx.doi.org/10.1021/es990903w. Retrieved.
Zarate, Erika, Carlos Belalcazar, Luis, Clappier, Alain, Manzi, V., Bergh, Hubert van den, 2007. Air quality modelling over Bogota city: combined techniques to estimate and evaluate emission inventories. Atmos. Environ. 41 (29), 6302–6318. Retrieved October 14, 2012. http://linkinghub.elsevier.com/retrieve/pii/S1352231007002403.
Zhang, Yanli, et al., 2015. Emission factors of fine particles, carbonaceous aerosols and traces gases from road vehicles: recent tests in an urban tunnel in the pearl river delta, China. Atmos. Environ. 122, 876–884. Retrieved August 17, 2017. http://linkinghub.elsevier.com/retrieve/pii/S1352231015302697.
Zhang, Yi, Stedman, Donald H., Bishop, Gary A., Guenther, Paul L., Beaton, Stuart P., 1995. Worldwide on-road vehicle exhaust emissions study by remote sensing. Environ. Sci. Technol. 29 (9), 2286–2294. http://dx.doi.org/10.1021/es00009a020. Retrieved.